Angewandte Chemie
Eine Zeitschrift der Gesellschaft Deutscher Chemiker

Supporting Information

69451 Weinheim, Germany

Using Ambient Ion Beams to Write Nanostructured Patterns for Surface Enhanced Raman Spectroscopy**

Anyin Li, Zane Baird, Soumabha Bag, Depanjan Sarkar, Anupama Prabhath, Thalappil Pradeep,* and R. Graham Cooks**

anie_201406660_sm_miscellaneous_information.pdf

Supporting Information

Contents

1. Experimental …… ..... p. 2
2. Enhancement factor calculations and uniformity evaluation…… ..... p. 4
3. SEM images of Ag^+ modified surfaces..... ……p. 10
4. Deposition plume: Spatial flux distribution, coverage, morphology and SERS signal ..... p. 14
5. Ion beam focusing to create surface patterns using metal electrolytic spray ionization deposition with masks…… ..... p. 16
6. References……...……p. 18

1. Experimental

Materials and Chemicals

The support surfaces used in this experiment included ITO slides, aluminum coated (~100 nm) microscope glass slides (Deposition Research Lab, St. Charles, MO), gold (120 nm) with titanium (100 nm) adhesion layer coated microscope glass slide (Deposition Research Lab, St. Charles, MO), ITO coated glass slides (1.1 mm thickness, 1" × 3", (Nanocs, New York, NY)), heavy duty aluminum foil of 0.01 mm thickness (Durable Packaging International, Wheeling, IL), soft annealed copper foil of 0.05 mm thickness (McMaster-Carr, Elmhurst, IL). Silver foil, stainless steel foils, and gold foil of 0.01 mm thickness were purchased from Aldrich Chemical Company (Milwaukee, WI). P400 silicon carbide abrasive paper (Buehler, IL) was used to remove oxide layer and roughen surfaces when needed. TEM grids (Electron Microscopy Science) were used as received.

The metal electrodes used for electrolytic spray ionization were assembled as previously described.[1] HPLC grade acetonitrile and methanol (Chromasolv, Sigma–Aldrich) were used as received. Crystal violet and Rhodamine 6G (reagent grade, Sigma–Aldrich) were used as received.

Chemical Instrumentation

A home-built ambient ionization and deposition set-up was used to accurately log the number of ions delivered onto any collection surface.[1] Briefly, a wire-in-acetonitrile nanoESI source was subjected to a high voltage of ~1.5 kV. The ionic species generated by the ion source were recorded using an Orbitrap mass spectrometer (LTQ Orbitrap XL, Thermo, CA) before and after deposition. Metal-containing ions were directed to a grounded target surface. The recombination current through ground was monitored and logged once a second. Target surfaces were grounded and positioned 5-10 mm away from the tip of the spray emitter under ambient conditions. Monolayer coverage (ML) was calculated based on the total deposited charge and the measured size of deposition spot using electron or optical microscopes. Perforated masks were used when focused ion beams or specific spot sizes were needed.

The spatial distribution of ion current at the deposition surface was measured using an IonCCD detector system (OI Analytical, College Station, TX, USA).[2] The IonCCD™ is a pixelated charge detector consisting of an array of 21 µm wide TiN pads or pixels 1.5 mm in height, separated by 3 µm. When ions come in contact with the floated electrode surface they are neutralized and their charge is stored over a user-determined integration time. Following integration the charge on each pixel is read out serially and the resulting signal is reported in the form of a digital number (dN). The detector array and associated electronics are housed in a stainless steel enclosure with a 1.5 mm wide, 49 mm long slit

exposed to the detector surface. A detailed description of the detector operation is provided by Hadjar et al.[3] Unless otherwise noted, the integration time was set to 100 ms with 25 V being applied to the stainless steel housing of the detector.

SEM images and EDAX data were taken on a FEI Philips XL-40 Scanning Electron Microscope with a Schottky field emission gun. High resolution TEM images of the samples were obtained using a JEOL 3010 instrument with a UHR pole piece. Specimens for TEM analysis were prepared by placing a lacey carbon grid on top of the collecting surface.

Several Raman instruments equipped with different lasers were used to evaluate prepared SERS active surfaces. The first instrument was an Alpha-SNOM 300 S confocal Raman microscope (WITec GmbH, Germany) with a 532 nm laser as excitation source. Large area scans (4 mm × 4 mm) used 200 spots per line. Large area optical images were taken using the image stitch option in the software of this Raman instrument. The second instrument was an Alpha 300 confocal Raman microscope (WITec GmbH, Germany) with a 633 nm laser as excitation source. The third instrument was a near Infrared Raman imaging microscope (Olympus BX60) equipped with a 785 nm laser. The fourth instrument was a home built portable Raman microscope equipped with 532 nm laser. Raman signals were collected using objective lenses, laser power intensities and with an integration times denoted individually in each figure.

All the Raman spectra shown here have been background-corrected. The background correction was done using the WITec instrument software, initially the spectrum was fitted with a best fit polynomial and then that was subtracted from the original spectra. Raman images were generated based on the intensity of Raman peaks using the WITec software.

2. Enhancement factor calculations and uniformity evaluation

The enhancement factor (EF) was calculated based on the measured Raman spectra. First the SERS intensities were compared with normal Raman intensities, corrected for the number of molecules under the laser spot. The formula to measure the EF is given as:[4]

$$EF = \frac{I_{SERS}/N_{surface}}{I_{normal}/N_{bulk}} \quad \text{..... (1)}$$

I_{SERS} and I_{normal} are the observed SERS intensities arising from the coating of analyte molecule (here, crystal violet (CV) or Rhodamine 6G (R6G)) on the Ag nanoparticle spot and the Raman intensity of analyte molecule in absence of nanoparticle (normal Raman signal). N_{bulk} and $N_{surface}$ are the number of analyte molecules excited under the laser spot for the bulk specimen and the number of analyte molecules under the laser spot on the Ag nanoparticles, respectively. In this report, I_{SERS} and I_{normal} were taken from the normalized (for power and acquisition time) intensity of Raman shift at 1176 cm^{-1} for CV and Raman shift of 1365cm^{-1} for R6G. $N_{surface}$ values are calculated using the formula given below:

$$N_{surface} = 4\pi r^2 \cdot C \cdot A \cdot N \quad \text{..... (2)}$$

where *r, C, A, N* are average particle radius of the Ag nanoparticles in the spot, surface density of the analyte monolayer, area of the laser spot and the average number of particles per square micrometer area, respectively. The average particle radius *r* was taken (from SEM measurement) as 32 nm, surface density of analyte molecule *C* was calculated as $10^5/\mu m^2$, the area of the laser spot (50× objective, Numerical Aperture = 0.55) diameter was 3 µm (A = 7.1μm^2), and the number of particles per square micrometer *N* from SEM measurement is 255.

N_{bulk} was calculated using the formula:

$$N_{bulk} = N_A \cdot A \cdot h \cdot \rho / M \quad \text{..... (3)}$$

where A is area of the laser spot, h is penetration depth of the laser, ρ is density of the solid analyte (0.83 g/cm^3 in case of crystal violet), molecular weight of the analyte (in this work, 408 for crystal violet and 479 for Rhodamine 6G). The laser spot was 3µm diameter; penetration depth of laser h was taken as 20 µm.

Using these parameters and the previously quoted equation (1-3), the highest EF for the AgNP structured copper foil was calculated to be 2×10^{10}, Fig. S1 (a). Table S1 summarizes the enhancement factor of AgNP spots on various support materials.

Molecular electronic resonance Raman (RR) and surface-enhanced Raman effects were observed to increase Raman signal synergistically. Crystal violet has a wide absorption spectrum with an absorption maximum ranging from 420 to 600nm depending on the environmental pH. The resonance Raman contribution to the enhancement factor (EF_{RR}) can be as much as $10^{5\sim7}$ when the laser wavelength matches the electronic excitation energy of the analytes.[5] This might be one reason for the extremely high signal intensity when crystal violet was probed using a 532 nm laser, as shown in Figure S1. This contributing factor complicates interpretation of the SERS enhancement factor.

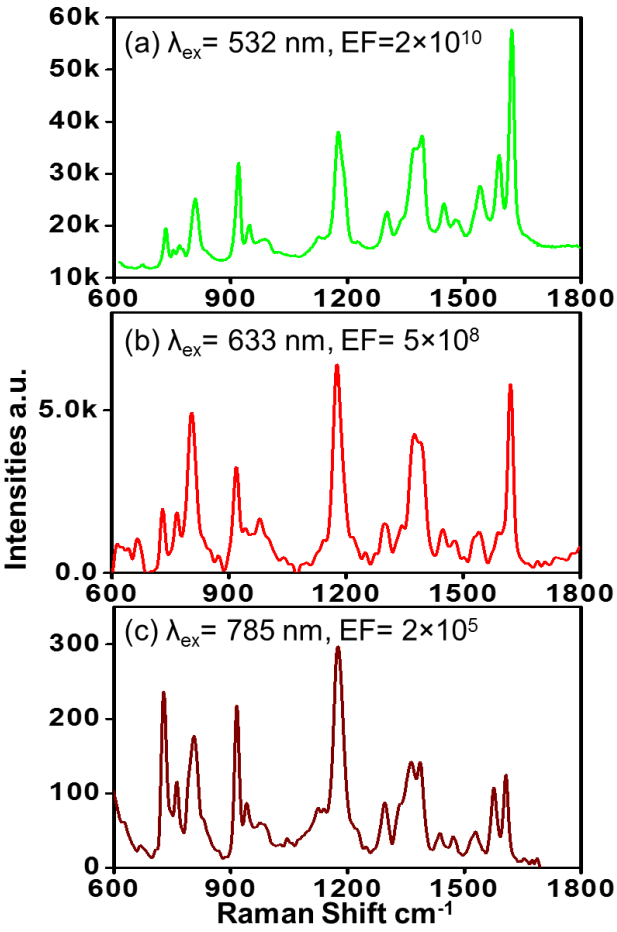

Figure S1. SERS spectra and average enhancement factor of crystal violet (10^5 per μm^2) on top of a AgNP nanostructure on copper foil substrate under excitation using (a) 532 nm, 20 mW (b) 633 nm, 8.6 mW (c) 785 nm, 52 mW laser sources. This is a copper foil surface modified by only ~7 ML of Ag ion, to avoid CCD saturation when using 532 nm laser.

The 785 nm laser is far away from the resonance of crystal violet. This experimental combination should give enhancement without interference of a resonance contribution. Fig. S1 (c) shows that the

near-IR laser gave an average enhancement factor of 2×10^5. The decrease of EF from 10^8, however, may also be due to the different interaction between created nanostructures with the near IR laser. For this reason, R6G was tested at 633 nm (which is far from R6G's resonance)[5a] for a better comparison. The result was intermediate but still a very high enhancement factor of ~1×10^8 was seen, as shown in Fig. S2.

Another interesting phenomenon observed in this SERS experiment is that the SERS signal always decreased while recording of the spectrum. If the sample was slightly moved, the signal would rise (sometimes beyond the CCD saturation level) to a high value and then immediately decrease within the 1 second integration time. In the imaging mode, the excitation laser was attenuated to 1 mW to avoid possible saturation. Raman signals were taken over each pixel with a 0.01 second integration time and then the sample stage was moved to next pixel. Much higher signal intensities, as well as enhancement factor were obtained in this short acquisition time imaging mode.

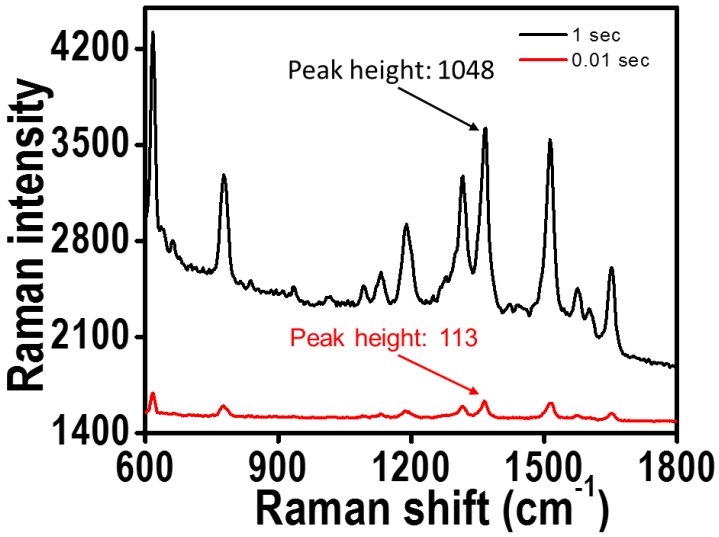

Figure S2. SERS spectra of R6G (10^5 per μm^2) on top of AgNP nanostructure on top of copper foil using excitation from a 1 mW, 633 nm laser. The two spectra were taken with (a) 1 second (b) 0.01 second recording time from the same spot region. The peak height (relative to baseline) of the 1365cm^{-1} band is labeled in both the spectra.

The above figure shows that the highest signal intensity found in the 1s integration scans is only 9 times higher than the highest signal intensity in 0.01 s integration scans. Similarly, when the laser power was turned down, the Raman signal decreased less than proportionately. For example, for the same substrate, the highest Raman intensity of 7,310 (Table S1) when the laser power was 8.6 mW only decreased to 4,253 when laser power was turned down to 1 mW. These phenomena could be the results of

thermal desorption of the molecule from the hotspot driven by laser heating, or the result of laser-induced melting of nanoparticles since no capping agent was used to protect the AgNPs. Even though the 0.01 integration time gave much better results, most of the EFs reported in Table S1 are based on 1 second integration time and with the consideration that most Raman spectrometers are built without image scanning functions. Also, for consistency, 8.6 mW laser power was also kept constant for the values in the Tables.

In summary, a resonance contribution may have increased the overall enhancement factor while laser induced damage could have decreased the actual enhancement factor. Future modifications to the surface may give even better performance for SERS applications.

SERS Uniformity of the modified surfaces

For high throughput SERS applications, surface uniformity is an important measure that determines the robustness of the experiment. Densely and evenly distributed hotspots would be ideal for rapid Raman analysis. In this experiment , the SERS uniformity of the modified surface within the same AgNP spot was evaluated by repeating measurements on randomly selected regions in that spot. The corresponding Raman signal intensity values from the AgNP spots on top of three different support materials were summarized in Table S1.

Table S1. SERS intensity of band 1176 cm^{-1} in different regions of spots created on different support materials, 10 ML Ag coverage, 8.6 mW, 633 nm laser excitation

Support Material	region 1	region 2	region 3	region 4	region 5	mean	%RSD
Copper Foil	9747	12733	11510	12921	11204	11623	11%
Al foil	2302	1213	2173	1690	1739	1823	24%
Au foil	7310	5324	4880	6160	5259	5787	17%

Another way to evaluate SERS uniformity is to take Raman images of the surface. Fig. S3 (a) shows a randomly selected AgNP array composed of small spots. Evaluation of uniformity was done by Raman imaging of the different areas composing the spot. As shown in the below Fig. S3 (b) and (c), these spots are effectively identical for SERS purposes.

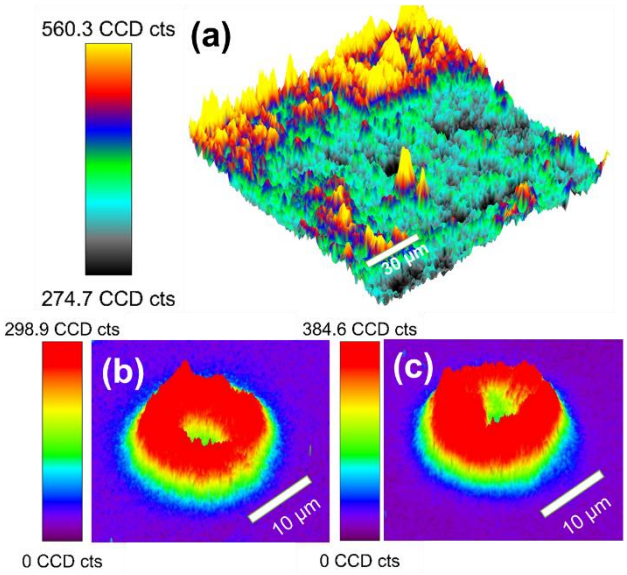

Figure S3. Raman images (3D plot viewed 45 degree angle) of (a) a randomly selected 150×150 μm^2 region in a ~3 mm AgNP spot (~5 ML on Cu foil); and two spots (b, c) in an array (Fig. S11). Crystal

violet (~10^5 per μm^2) was applied over the whole region by dropcasting a solution onto the copper foil. The images were generated using the 1176 cm^{-1} peak intensity of crystal violet (using 1 mW, 633 nm laser excitation, and acquisition time of 0.01 second). The SERS uniformity within the bigger spot gave a maximum-minimum difference of only ~50% in a randomly selected 150×150 μm^2 region. The SERS uniformity of smaller array spots is demonstrated by the similarity (in shape and intensity) of the Raman images of CV from two randomly selected spots in the array pattern. The volcano shape of the Raman imaging might be due to the flux distribution in the depositing ion plume when focused to 20 μm.

There was no detectable change in surface activity when storing a substrate in air for three days. Even after 1 month, there was still ~10% activity for the surfaces. For an uncapped NP this is highly satisfactory. We believe that the surface anchoring contributes to the stability. In summary, the net enhancement signal is highly uniform, especially when considering the variation in the surface distribution of the analyte brought about by dropcasting.

3. SEM images of Ag^+ modified surfaces

A series of surfaces was tested as supported materials for in situ preparation of AgNP by metal electrolytic spray ionization deposition. Different SERS performance was found for the different support materials as summarized in Table S2. These modified surfaces show different morphologies as imaged by scanning electron microscope. Even among the "good" substrates, different morphologies can be observed. Interestingly, the SERS surfaces retained >10% activity after exposure to SEM analysis.

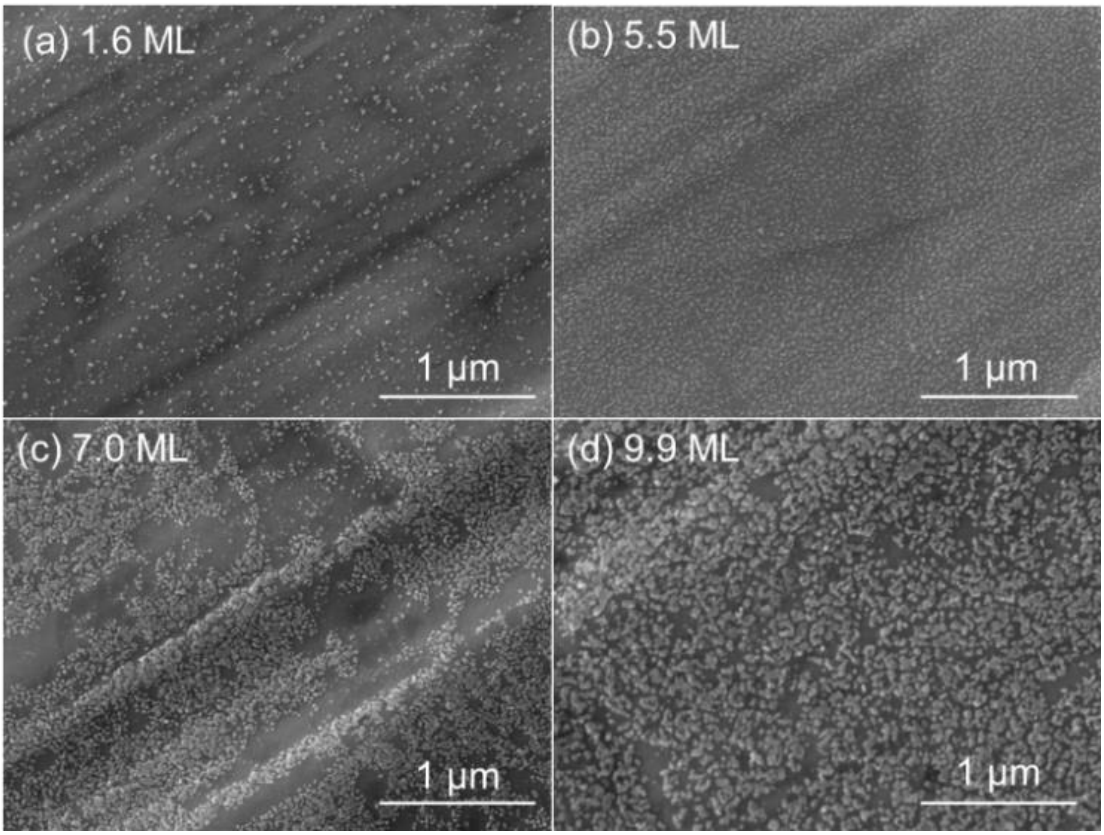

Figure S4. Morphologies of surface nanostructures created by depositing different amounts of silver ions onto a copper foil using metal electrolytic spray ionization deposition. Coverage turned out to be one determining factor for the SERS performance of spots created by this surface modification method.

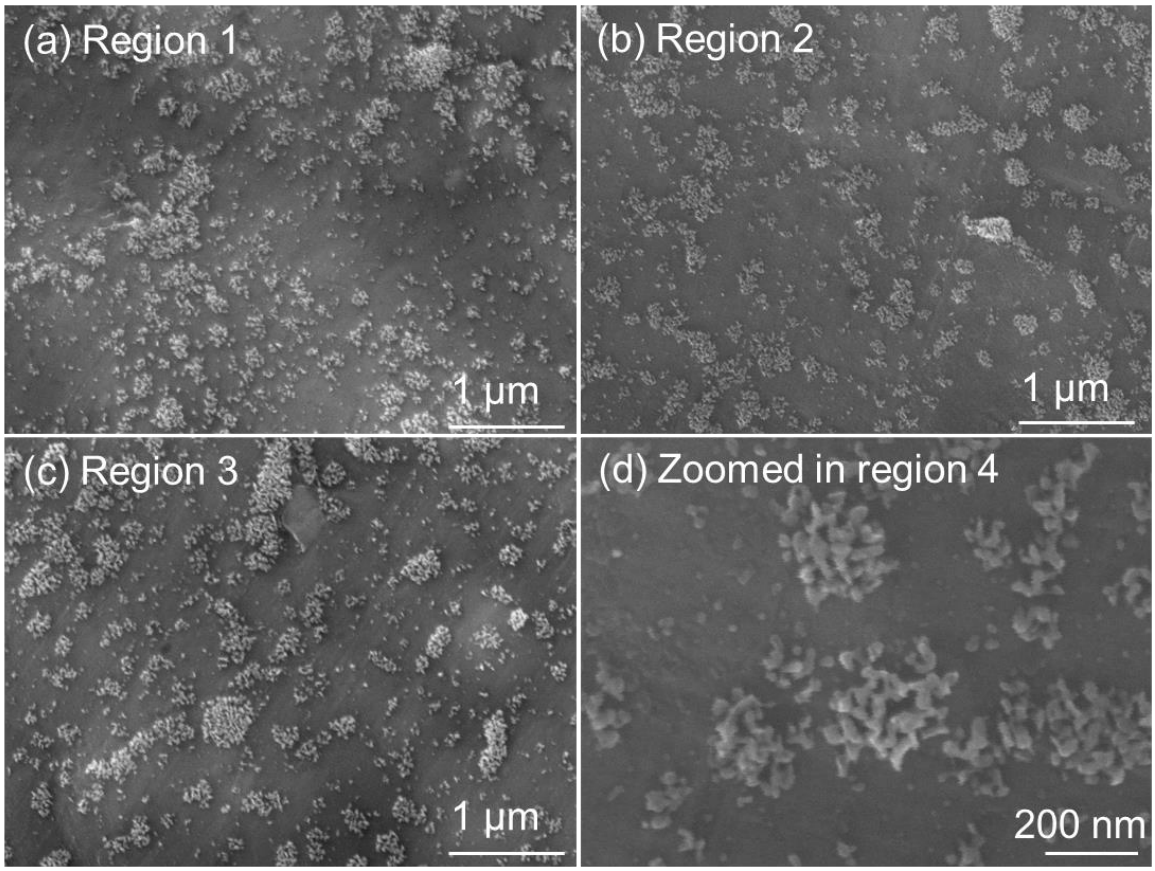

Figure S5. AgNP structures created by 10 monolayer coverage of Ag^{+} deposited onto aluminum foil. Polydispersed morphology was uniform throughout each spot created. (a), (b), (c) and (d) are images from four randomly selected regions located >200 μm from each other in the same deposition spot.

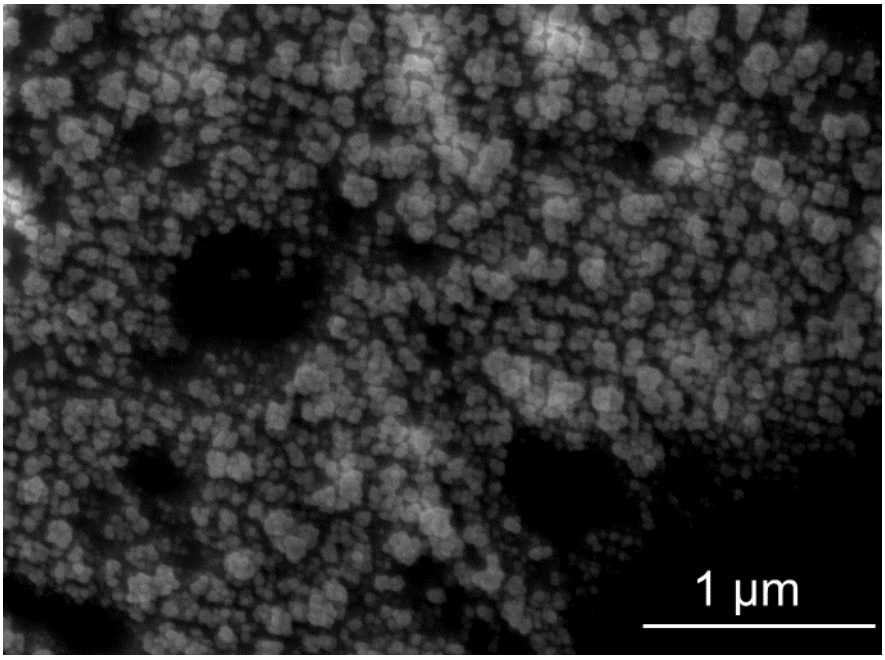

Figure S6. AgNP structures created by 10 monolayer coverage of Ag^{+} deposited onto gold foil.

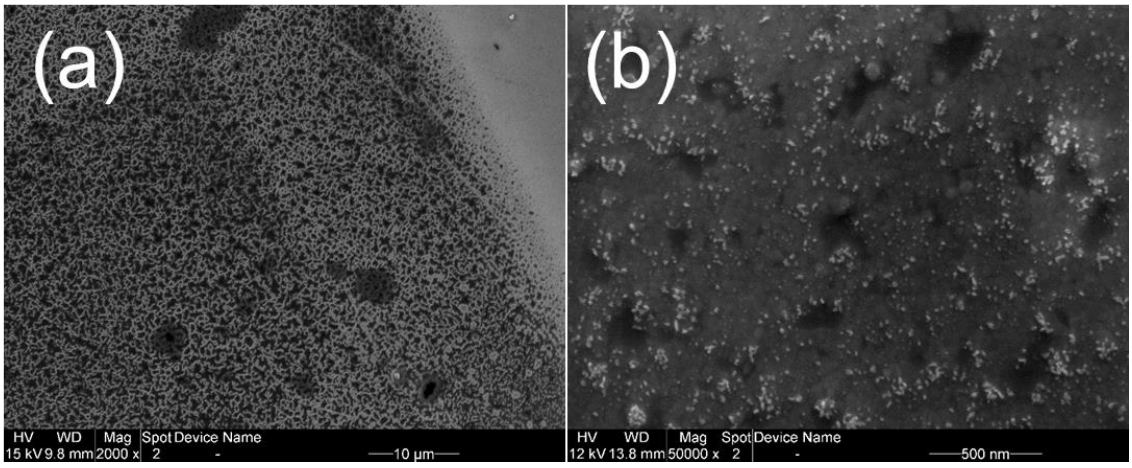

Figure S7. AgNP structures created by on top of (a) ITO coated slide and (b) aluminum coated glass slide. The AgNP nanostructures created on these polished flat surfaces do not give high quality SERS data at silver coverage 1-20 ML. Nanostructures created on these surfaces are either aggregates which are too large or individual particles are too small to have appropriately sized nano gaps.

Table S2. SERS intensity of band 1176 cm^{-1} of CV on AgNP spots created on different support materials (~10 ML Ag coverage), 8.6 mW, 633 nm laser excitation and 1 second acquisition time.

Support Material	Highest Peak Intensity (1176 cm^{-1})	Enhancement Factor
Copper Foil	12921	4E8
Gold foil	7310	2E8
Aluminum Foil	2302	7E7
Copper Tape	3731	1E8
Brass foil	40	1E6
Stainless Steel Foil	181	5E6
Silver foil	N. A.	N.A.
ITO coated slide	30	8E5
Aluminum coated slide	N.A.	N.A.
Penny coin, AgNP first	590	2E7
Penny coin, Sample first	471	1E7

4. Deposition plume: Spatial flux distribution, coverage, morphology and SERS signal

Once loaded with anhydrous acetonitrile and in contact with the high voltage, the metal electrolytic spray ionization source readily generated silver-containing ions as the dominant ion signal as observed using an atmospheric pressure sampling mass analyzer.[1] The diameter of the charged droplet emitter tips was typically 1-5 μm. After moving in ambient air along the electric gradient for ~5 mm, the spray plume diameter expanded to 1-5 mm. The metal ion distribution in this expanded plume may result in an uneven distribution of precursor ion concentrations on the collecting surface. When mapped using an Ion CCD (Fig. S7 (a) and (b)), a spray plume of ~3 mm diameter showed the maximum current in the center dropping slowly to less than 30% in the first 1.5 mm from the center. For the next 1 mm, the current dropped a lot more rapidly and accounted for the remaining 70% of the signal. For this reason, we assume a uniform distribution of deposited metal ions across most of the area inside the deposition circle. This "uniform in the center" assumption is largely valid as observed by optical and electron microscopes. Coverage can be controlled by deposition time with an estimation based on deposition current and spot size. The actual coverage of each experiment was calculated afterwards with the accurately measured spot sizes and the deposition currents logged by a computerized system.

$$Coverage = (\frac{N_A}{A \cdot F} \sum Idt)/ML$$

A is the measured spot area, F is the Faraday constant, N_A is the Avogadro constant, I is logged landing current, dt is the logging interval. ML is the monolayer atom density for silver, 1.6×10^{15} atom/cm^2.

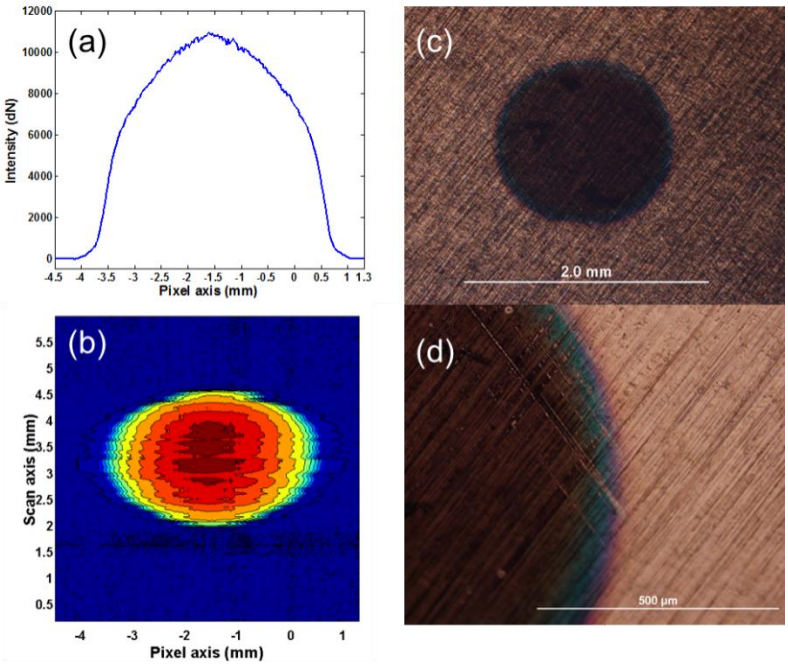

Figure S8. (a) A cross section scan and (b) the reconstructed contour plot of the ion intensity at the deposition surface as measured by the scan of the ionCCD. The elongation along the x-axis of the figure is due to distortion caused by the distance (1.5 mm) between the entrance slit and the detector boards. (c) Spot created by depositing silver ions for 12 hours with an average coverage of 100 ML. (d) On the edge of this spot, where the actual coverage varied due to the current density drop, rainbow-like color transition was observed. This means that the surface plasmon resonance of this modified surface area can be roughly tuned by **just** varying the coverage of depositing silver ions between 0 and 100 ML.

5. Ion beam focusing and creation of surface patterns using metal electrolytic spray ionization deposition with masks

Static patterns of nanoparticle containing spots were created by putting masks between the ion emitter and the deposition targets. Grounded conductive masks create a negative pattern by simply blocking ion deposition on the positive regions. Non-conductive and floated conductive masks, however, provides additional focusing effect that gives higher flux and smaller (than the mask holes' dimensions) spots.

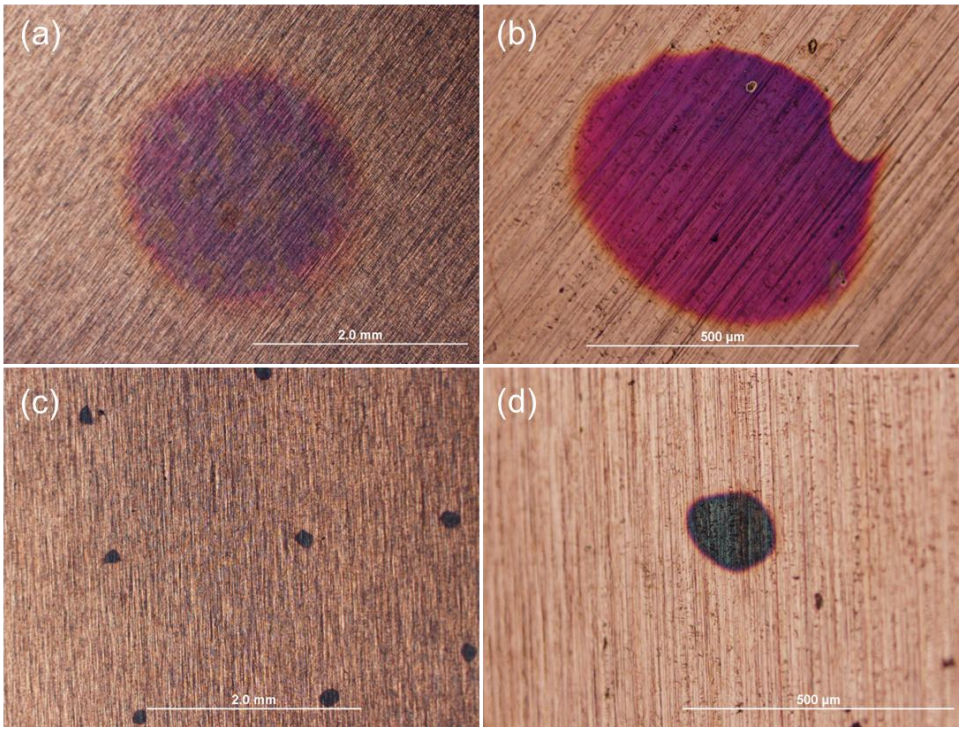

Figure S9. (a) AgNP spot 4.9 mm^2 created on copper foil by direct deposition without using any focusing or masking. This spot of averaged 8 ML coverage of silver was created by 136min deposition of 13 nA landing current. (b) Using a perforated plastic tape mask (50 µm thick, ~500µm diameter) on top of the deposition target, only 17 min of deposition was needed to get twice as much coverage for this 0.23 mm^2 spot even though the total depositing current dropped to 8 nA. Improved color uniformity was also achieved by this spot compared to (a). (c) An array of even smaller spots was created by using an arrayed mask. This dark green color is from ~ 50 ML coverage. 100 µm spots (d) separate by < 2 mm is as good as hand-craftsmanship can get.

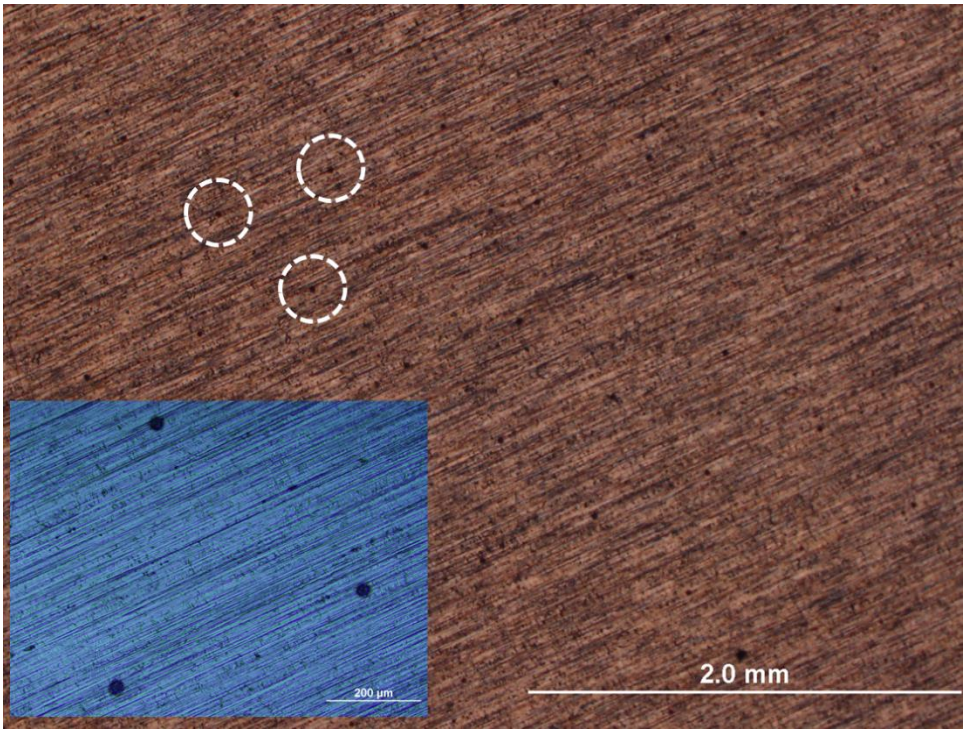

Figure S10. An array of AgNP spots deposited on top of a copper foil using a floated conductive stainless steel mesh as mask. The spots are 560µm away from each other. The uniform 20 µm spots are created by mask with 200 µm holes shown in the Fig. S11. This type of focusing might be useful for further downsizing the fabrication dimensions. The SERS activity of these spots is seen from the images in Fig. S3.

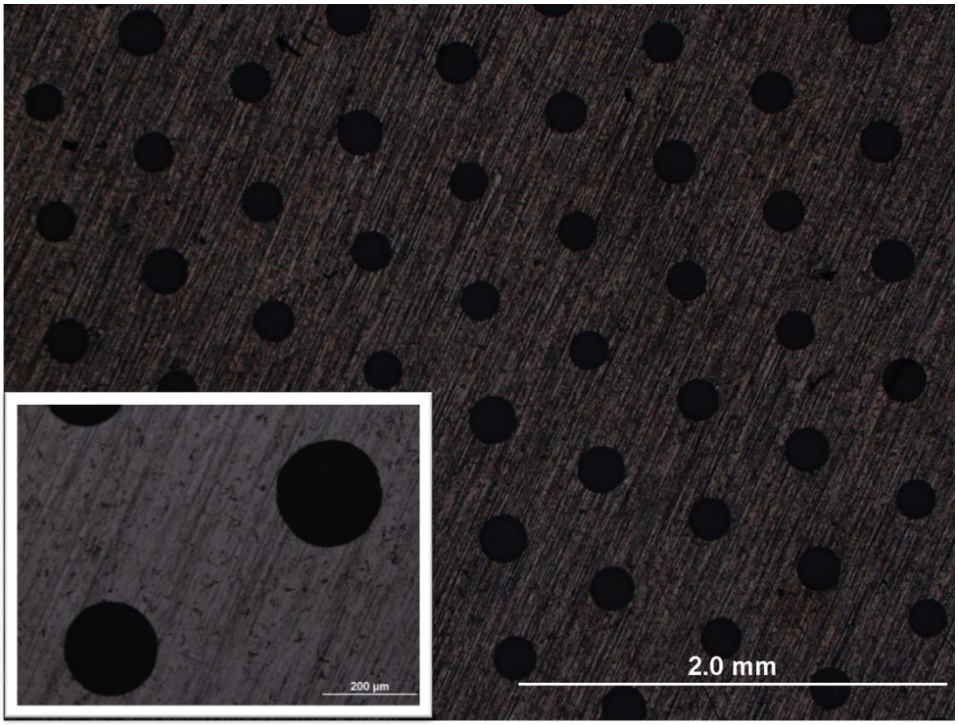

Figure S11. Stainless mesh used to create the pattern shown in Fig. S10. This mesh is a flat 200 µm thick plate composed of with ~200 µm holes. The floating/insulation from ground is achieved by 50 µm separation with the deposition target.

References:

[1] A. Li, Q. Luo, S.-J. Park, R. G. Cooks, *Angew. Chem., Int. Ed.* **2014**, *53*, 3147-3150.
[2] Z. Baird, W. P. Peng, R. G. Cooks, *Int. J. Mass Spectrom.* **2012**, *330*, 277-284.
[3] O. Hadjar, G. Johnson, J. Laskin, G. Kibelka, S. Shill, K. Kuhn, C. Cameron, S. Kassan, *J. Am. Soc. Mass Spectrom.* **2011**, *22*, 612-623.
[4] P. L. Stiles, J. A. Dieringer, N. C. Shah, R. P. Van Duyne, *Annu. Rev. Anal. Chem.* **2008**, *1*, 601-626.
[5] (a) J. A. Dieringer, K. L. Wustholz, D. J. Masiello, J. P. Camden, S. L. Kleinman, G. C. Schatz, R. P. Van Duyne, *J. Am. Chem. Soc.* **2009**, *131*, 849-854; (b) S. L. Kleinman, E. Ringe, N. Valley, K. L. Wustholz, E. Phillips, K. A. Scheidt, G. C. Schatz, R. P. Van Duyne, *J. Am. Chem. Soc.* **2011**, *133*, 4115-4122.